Observing boreal wildfire impacts on HCHO and NO_2 from space

K. Lapina[1,4], R. Honrath[1], R. C. Owen[1], A. Richter[2], F. Wittrock[2], E. Hyer[3] and J. P. Burrows[2]

[1]Michigan Technological University, USA, [2] Naval Research Laboratory, USA, [3]University of Bremen, Bremen, Germany, [4] Colorado State University, USA

ABSTRACT

We use tropospheric column data from SCIAMACHY (Scanning Imaging Absorption spectrometer for Atmospheric CHartographY) together with the Lagrangian particle transport model FLEXPART simulations of boreal wildfire emissions from BWEM (the Boreal Wildland-Fire Emissions Model) inventory to study the impact of 2004 Alaskan and Canadian fires on HCHO and NO_2 levels in the North American boreal region.

Main conclusions:

- HCHO burden in the plumes up to 2 days old was dominated by fires.
- Secondary HCHO production lasted for at least 2 days after the release of fire emissions.
- Fires had a moderate impact on NO_2, which had other important sources in the region.

METHODS

SCIAMACHY

SCIAMACHY is an absorption spectrometer covering the spectral range from the UV to the NIR, with an equator crossing time of 10 AM LT. The details on retrieval techniques and error analysis can be found in works [2] and [3]. Due to the patchy observations (global coverage is achieved within 6 days) we used 5-day composites in this study (Fig. 1).

Selection of plume region

FLEXPART [4] was used to simulate the advection and dispersion of HCHO and NO_x fire emissions. Analysis of the fire impact on HCHO and NO_2 was performed for the transported plume regions, identified by the model. The maximum age for the HCHO and NO_2 fire tracers were 48 and 6 hours, respectively. FLEXPART output at 18 UTC, the mean satellite overpass time in the region (~10 AM in Alaska), was sampled only at the locations coincident with satellite measurements and combined to obtain 5-day composites.

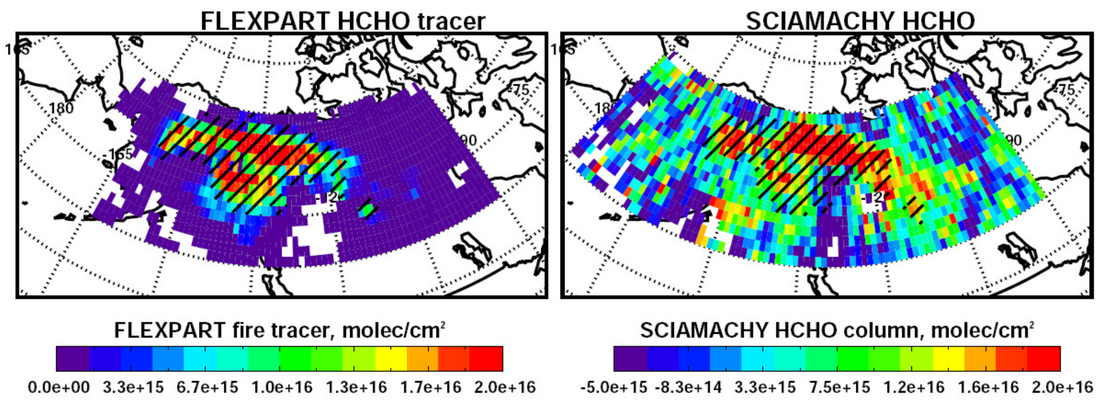

Figure 1. An example 5-day 1º x 1º composites (July 11-July 15) of FLEXPART HCHO tracer simulations (left) and HCHO SCIAMACHY trop. columns (right). The plume region defined based on high value of the fire HCHO tracer is hatched in black. White areas within the study region indicate either zero tracer concentrations (for FLEXPART only) or missing satellite data.

HCHO and NO_2 burden calculation

We define burden of the plume as the total mass of HCHO or NO_2 contained in the plume region, and calculated as

$$B = k\sum_i a_i \times C_i \qquad (1)$$

where B is the burden (in Gg), a_i is area of the grid cell i, C_i is a SCIAMACHY or FLEXPART-derived trop. column (molec/cm^2) in cell i, and k is a unit conversion factor.

Contributions to the HCHO burden in fire plumes

The total HCHO burden in the plume, **B**, can be separated into the burden enhancement due to fires and the background burden, $\mathbf{B_{bk}}$:

$$B = B_{bk} + B_{direct} + B_{\text{secondary}} \qquad (2)$$

where $\mathbf{B_{direct}}$ is the contribution of primary HCHO emissions, and $\mathbf{B_{secondary}}$ is the burden resulting from secondary HCHO production from VOCs emitted from fires. $\mathbf{B_{bk}}$ was estimated by determining the HCHO burden corresponding to an area of the same size as each plume, but not containing fire emissions. For every composite this was done by randomly selecting background locations (300 grid cells) at a significant distance away from the fire sources, based on low values of the HCHO fire tracer. Their burden per unit area was multiplied by the area of the plume to obtain $\mathbf{B_{bk}}$ for that composite. HCHO columns for background cells exhibited large variability (Fig. 2) due to noise in the SCIAMACHY data.

To estimate $\mathbf{B_{direct}}$, we used the FLEXPART age spectra to define the distribution of times since emission and reduced the contributions of emitted HCHO according to the HCHO destruction rate constant between the release time, t_E, and the time of measurement, t_M. The total burden in grid cell j can be obtained by summing up incremental contributions over all values of Δt:

$$B_{direct_j} = \sum_{t_M - \infty}^{t_M} A_{0,t_E} \exp(-k'\Delta t) \qquad (3)$$

where $A_{0,\,tE}$ is the contribution of emissions Δt time upwind in the absence of removal, and k' is a diurnally varying (between a maximum daytime value and zero at night) rate constant for a pseudo-first order reaction for HCHO removal. Maximum k' was selected based on the estimates of the column-averaged τ (with τ defined as 1/k') at overhead conditions ranging between 1.5 and 3 hours [8, 9].

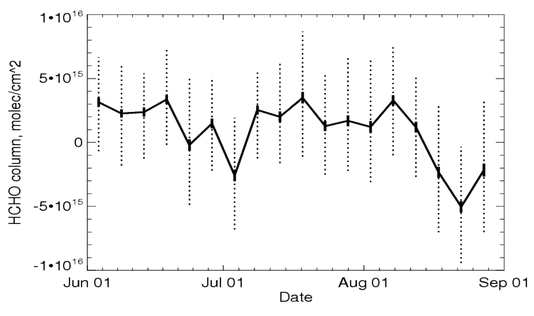

Figure 2. Mean HCHO trop. background column for each of the 5-day HCHO composites. Mean +/- std. error of the mean is shown with solid vertical lines and the 25th and 75th percentiles of the HCHO data are shown with the dotted lines.

The Boreal Wildland-Fire Emissions Model (BWEM)

BWEM [5] was used to estimate HCHO and NO_x emissions. Main features of the model:

- Emissions are estimated separately for burning of aboveground vegetation (at a ratio of 80% flaming/20% smoldering) and surface organic layer (at a ratio of 20% flaming/80% smoldering).
- Depth of surface layer burning for August is twice the depth for June – July, resulting in increase in emissions, especially for smoldering compounds.
- Emissions were calculated by applying emission factors (EF). For HCHO: EF_{smol}=5.3 and EF_{flam}=2.6 g HCHO/kg C (corresponds to overall EF of 1.85±0.38 g HCHO/kg fuel [6]). For NO_x EF_{smol}=5.64 and EF_{flam}=1.24 g NO_x as NO/kg C.
- Daily emissions were calculated on a 1º x 1º. Source for area burned and locations: Fire Service (Alaska) and Forest Service and MODIS (Canada). Fire temporal distribution: MODIS.

RESULTS AND DISCUSSION

Fig. 3a presents early-to mid-June HCHO and NO_2 composites (left and center) and total BWEM CO emissions (right), for the period prior to the start of the main fire season. Large increases in HCHO columns are noticeable later in the summer (Fig. 3b-d).

Figure 3. Composites of HCHO (left), NO_2 (center) and total BWEM CO emissions over fire locations (right) for the 19-day periods in 2004. Black borders (right images) show the study region (55-70N, 180-90W).

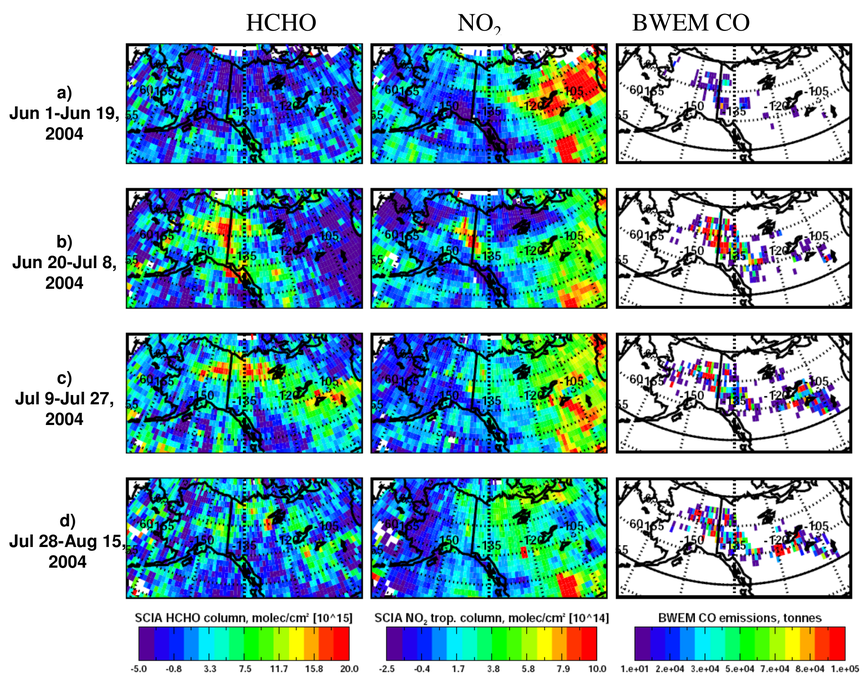

Plumes were identified for 13 out of 18 composites. The emissions and transport models performed well overall, and simulations agreed with observations on 15 out of 18 periods. During the periods with significant fire activity most of the HCHO mass is contained within the plume region (Fig. 4).

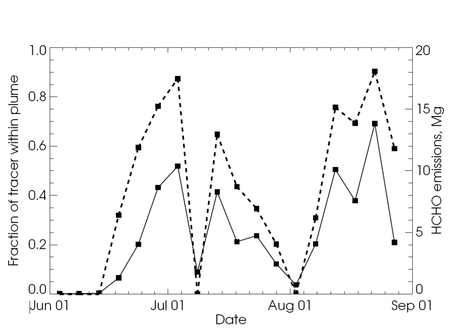

Figure 4. Fraction of HCHO tracer mass contained within the plume area (dashed line) and total 5-day average daily BWEM emissions of HCHO (solid line).

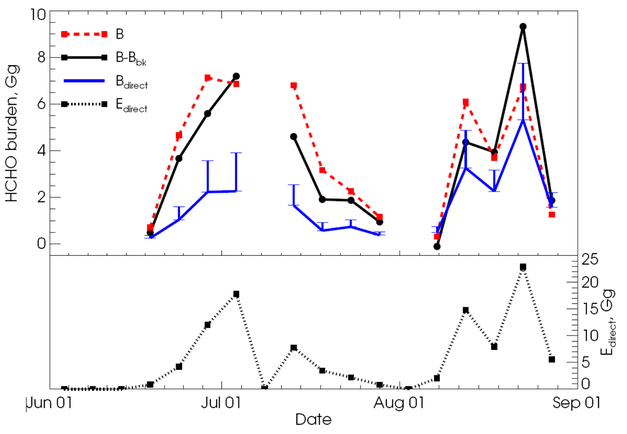

Figure 5. HCHO burdens in the identified fire plumes in each 5-day composite and total emissions contributing to the fire plumes.

Fig. 5 presents the SCIAMACHY-estimated fire burdens ($B-B_{bk}$, solid black line) in the transported fire plumes in each 5-day composite. The correlation between fire burden and the total fire emissions contributing to the transported plumes (dotted black line), was high (R=0.91), implying that fires greatly affected HCHO levels over the plume regions. The total HCHO burden in the fire plumes (B, red dashed line) also tracked the variations in emissions relatively well (R=0.82), consistent with the expectation that fires were the major source of variability in HCHO columns in the identified plume regions. The blue line with error bars in Fig. 5 shows B_{direct}, the burden contribution due to directly released HCHO emissions, calculated using eq. 3 with two different estimates of k'_{max}. The significant difference between the fire burden ($B-B_{bk}$) and B_{direct} indicates a considerable contribution of secondary HCHO.

Fig. 6 shows $B_{secondary}$ plotted against total HCHO emissions released over the 48-hour period preceding the measurement and transported with the fire plume. $B_{secondary}$ was rather well correlated to emissions (R = 0.75). This may be explained as a result of the fact that HCHO emissions are approximately proportional to the amount of the fire-emitted VOCs.

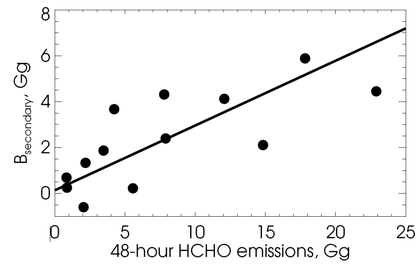

Figure 6. Contribution of secondary HCHO production to the HCHO burden in the plume regions, $B_{secondary}$, versus HCHO emissions released over the previous 48 hours.

CONCLUSIONS

- Fires dominated the HCHO burden in regions affected by emissions of up to 2 days upwind and high HCHO in fire plumes was sustained for at least 48 hours, due to continuing secondary production from the fire-emitted VOCs.
- We estimated that at least 0.6 – 1.3 Tg of HCHO was added to the atmosphere from the Alaskan and Canadian fires in 2004. The magnitude of HCHO secondary production was comparable to the burden due to the directly released HCHO.
- Fires had a moderate effect on NO_2 burden in fire plumes, and sources other than fires dominated NO_2 column amounts in the study region.

REFERENCES

1.Stavrakou, J. et al (2009) , Evaluating the performance of pyrogenic and biogenic emissions inventories against one decade of space-based HCHO columns, ACP, 9(3), 1037-1060
2.Wittrock , F. (2006) , The retrieval of oxygenated volatile organic compounds by remote sensing techniques, Ph.D. thesis, 192 pp., Univ. of Bremen
3.Richter, A. et al (2005), Increase in tropospheric nitrogen dioxide over China observed from space, Nature, (437), doi: 0.1038. nature04092
4. Stohl, A.et al (2005) Technical note: The Lagrangian particle dispersion transport model FLEXPART version 6.2, ACP, 5, 2461-2474
5.Kasischke, E. S., et al. (2005), Influences of boreal fire emissions on Northern Hemisphere atmospheric carbon and carbon monoxide, GBC, 19, GB1012, doi: 10.1029/2004GB002300
6.Goode, J. G., et al. (2000), Measurements of excess O3, CO, CH4, C2H4, C2H2, HCN, NO, NH3 , HCOOH, CH3COOH, HCHO, and CH3OH in 1997 Alaskan biomass burning plumes by airborne Fourier transform infrared spectroscopy (AFTIR), JGR, 105(D17), 22,147–22,166, doi:10.1029/2000JD900287
7. Wittrock , F. et al. (2006), Simultaneous global observations of glyoxal and formaldehyde from space, GRL, 33, L16804, doi:10.1029/2006GL026310
8. Macdonald, A. et al. (2001), Summertime formaldehyde at a high-elevation site in Quebec, (106), D23, pp 32,361-32,374

ACKNOWLEDGEMENTS

This work was supported by National Science Foundation grant ATM-0535486.

Michigan Technological University